Decomposition of Long-chain Petroleum Hydrocarbons by Fenton-like Processes: Effects of Ferrous Iron Source, Salinity and Temperature

Junhao Qin[1,2], Chuxia Lin[2*], Hamad Almebayedh[2] and Meshari Albader[3]

[1]Key Laboratory of Agro-Environment in the Tropics, Ministry of Agriculture of the People's Republic of China, South China Agricultural University, Guangzhou, 510642, China

[2] School of Environment and Life Science, University of Salford, Greater Manchester M5 4WT United Kingdom

[3]Kuwait Oil Company, Al Ahmadi 61008 Kuwait

Corresponding author; email: C.Lin@salford.ac.uk

ABSTRACT

Batch experiments were conducted to examine the effects of ferrous iron source, soil salinity of temperature on degradation of long-chain petroleum hydrocarbons by Fenton-like processes. The results show that over 70%, 50% and 25% of aliphatic C16-C21, C21-C35 and C35-C40, respectively, was eliminated at a H_2O_2 dose of 1.5%. The decomposition rate of petroleum hydrocarbons was similar to each other for ferrous sulfate and magnetite while the capacity of pyrite to trigger Fenton-driven decomposition of long-chain aliphatic petroleum hydrocarbons was weaker, as compared to ferrous sulfate and magnetite. The decomposition rate of aromatic hydrocarbons decreased with increasing length of carbon chain in the ferrous sulfate and magnetite systems, but the opposite was observed in the pyrite system. The effect of Fenton-like process on degradation of long-chain petroleum hydrocarbons was enhanced by increased temperature. At a temperature of 60^{o}C, the enhancement of Fenton process outweighed the adverse effects from potential loss of H_2O_2 due to elevated temperature. The use of magnetite as a source of ferrous iron was likely to prevent consumption of Fe^{2+} by complexation with chloride ion from occurring and consequently effectively eliminated the inhibitory effect of salinity on Fenton reaction.

Keywords: Oil contamination, chemical degradation, hydrogen peroxide, hydroxyl radical, desert, saline soil,

1 Introduction

The use of petroleum as a major source of energy supply in the past decades has resulted in widespread soil contamination around the world (Hall et al., 2003; Vieira et al., 2007; Safdari et al., 2018). This prompts increasing effort to develop methods for cleaning up petroleum hydrocarbon-contaminated soils. Bioremediation is thought to be a cost-effective method for remediating petroleum hydrocarbon-contaminated soils (Varjani et al., 2017; Li et al., 2018). However, the operation of bioremediation requires favourable environmental conditions for the hydrocarbon-degrading microbes. In desert areas where soil moisture and nutrients are lacking, microbially mediated degradation of petroleum hydrocarbons is generally inhibited. High soil salinity and temperature can also be limiting factors for soil bioremediation (Rhykerd et al., 1995; Margesin et al., 2001; Zhu et al., 2017). To allow bioremediation to be operated in these areas, manipulation of growing environments for microbial degraders such as supply of fresh water, cooling, fertilization and de-salinization of soil is required. This could add markedly to the operational costs associated with bioremediation and make it economically unviable.

Alternatively, advanced oxidation methods based on Fenton or Fenton-like process may have advantage over bioremediation for treatment of petroleum hydrocarbon-contaminated soils in desert areas given that no highly environment-sensitive biota are involved in these treatment processes. While advanced oxidation is a well-established method for degradation of organic molecules (Bissey et al., 2006; Bach et al., 2010; Maizel et al., 2017), there has been limited work reported for its application to decomposition of long-chain petroleum hydrocarbons, which frequently dominate aged soil-borne hydrocarbons in most desert environments due to rapid volatilization of the lighter components. Little is known about the influence of salinity and temperature on the effectiveness of Fenton or Fenton-like processes for chemical degradation of long-chain hydrocarbons. Furthermore, to increase the cost-effectiveness of the advanced oxidation process, identification of cheap but

effective ferrous iron-bearing materials is also important. The objectives of this study were to (a) compare the effectiveness of various ferrous iron-containing materials for Fenton-driven decomposition of long-chain petroleum hydrocarbons; (b) examine the effects of salinity on the degradation reactions; and (c) examine the effects of temperature on the degradation reactions.

2 Materials and Methods

2.1 Ferrous iron-containing materials

Three ferrous iron-containing materials were used in this study: (1) analytical grade ferrous sulfate ($FeSO_4 \cdot 7H_2O$), (2) powdered pyrite (FeS_2) with a diameter <75 μm, and (3) powdered magnetite (Fe_3O_4) with a diameter <18 μm. The powered pyrite and magnetite were purchased from Yunkai Powder Co., Ltd. and Guotao Mine Product Trade Co., Ltd., respectively.

2.2 Artificially contaminated soils

The synthetic petroleum hydrocarbon-contaminated soils were formulated by thoroughly mixing quartz sands (<38 μm) with a range of long-chain hydrocarbon species purchased from Sigma-Aldrich. This artificially contaminated soil contained 5000 mg/kg of eicosane (purity: 99 %), 6500 mg/kg of tetracosane (purity: 99 %), octacosane (purity: 99 %) and dotriacontane (purity: 97 %), 3000 mg/kg of hexatriacontane (purity: 98 %), 5000 mg/kg of naphthalene (purity: 99 %), acenaphthene (purity: 99 %), phenanthrene (purity: 98 %) and pyrene (purity: 98 %).

2.3 Experiment 1: Comparison between different ferrous iron-containing materials

A batch experiment was conducted to compare the effects of ferrous sulfate, pyrite and magnetite on the decomposition of the hydrocarbons in the synthetic soils. For each ferrous iron-containing material, one control and three treatments were set. The ingredients for the controls and various treatments are given in Table 1. 100 mL plastic bottles were used as batch reactors. After

placing all the solid components in the batch reactor, 50 mL of a relevant H_2O_2 solution was added into the reactor. The reaction was allowed to proceed until the reaction was completed, as indicated by no visible gas bubbles being observed. The soil was then freeze-dried using a 40 freeze-dryer.

Table 1 Experimental set-up for comparison between different ferrous iron-containing materials

	Contaminated soil (g)	$FeSO_4 \cdot 7H_2O$ (g)	Pyrite (g)	Magnetite (g)	50 mL of H_2O_2
CFS	50	4.5322			0%
T1FS	50	4.5322			0.5%
T2FS	50	4.5322			1%
T3FS	50	4.5322			1.5%
CP	50		1.9559		0%
T1P	50		1.9559		0.5%
T2P	50		1.9559		1%
T3P	50		1.9559		1.5%
CM	50			3.77	0%
T1M	50			3.77	0.5%
T2M	50			3.77	1%
T3M	50			3.77	1.5%

2.4 Experiment 2: Effects of salinity and temperature on degradation reaction

For this experiment, only magnetite was used. The dose of H_2O_2 was also fixed to 1.5%. The amount of contaminated soil and magnetite used in the experiment was the same as in Experiment 1. Two levels of salinity and two levels of temperature were set, as shown in Table 2. 100 mL plastic bottles were used as batch reactors. After placing all the solid components in the batch reactor, 50 mL of H_2O_2 solution was added into the reactor. The reaction was allowed to proceed in two ovens with one set at 35°C and another set at 60°C. After the reaction was completed, as indicated by no visible gas bubbles being observed. The soil was then freeze-dried using a 40 freeze-dryer.

Table 2 Experimental set-up for effects of salinity and temperature on degradation reaction

	Contaminated soil (g)	Magnetite (g)	Temperature (^{o}C)	NaCl (g)	50 mL of H_2O_2
CT35S1.5	50	3.77	35	0.8188	0
CT35S3.0	50	3.77	35	1.6376	0
CT60S1.5	50	3.77	60	0.8188	0
CT60S3.0	50	3.77	60	1.6376	0
TT35S1.5	50	3.77	35	0.8188	1.5%
TT35S3.0	50	3.77	35	1.6376	1.5%
TT60S1.5	50	3.77	60	0.8188	1.5%
TT60S3.0	50	3.77	60	1.6376	1.5%

2.5 Analytical Methods

The petroleum hydrocarbons contained in the soils were extracted with dichloromethane. Impurities are removed from the extract with sodium sulfate and silica. The aliphatic and aromatic fractions are separated using solid-phase extraction techniques. Additional clean-up for the extract was performed by passing the solution through a membrane filter. The filtrate was treated with 15 g of acid silica in a clean round bottom flask placed on a rotary evaporator with no heat for 30 min. The solution is then analyzed using a capillary gas chromatography with flame ionization detection (GC/FID) method (Weisman, 1998). The analysis was performed in an accredited commercial analytical laboratory (Concept Life Sciences Analytical & Development Services Limited).

2.6 QC/QA and Statistical analysis

Analytical quality control is maintained by a number of measures. Multi-point calibration was performed with authentic standards (with defined minimum performance characteristics). Independent standards, matrix spikes or reference materials were used for each analytical batch.

Statistical significance analysis was performed using One-way ANOVA (SPSS22.0). Repeatability analysis shows that the mean RSD was 4.79% for aliphatic C16-C21 fraction, 4.92%

for aliphatic C21-C35 fraction, 4.65% for aliphatic C35-C40 fraction, 2.55% for aromatic C10-C12 fraction, 3.14% for C12-C16 fraction, and 3.06% for aromatic C16-C21 fraction.

3 Results

3.1 Various Residual Aliphatic Hydrocarbons Using Different Fe^{2+} source

For the C16-C21 fraction, there was no significant difference among the three controls (CFS, CM and CP). For each of the 3 Fe^{2+} sources, there was a clear trend that the residual hydrocarbon decreased with increasing H_2O_2 dose at a statistically significant level (p<0.05) except for CP vs T1P where no statistical significance was observed (Table 3).

Table 3 Concentration of various residual aliphatic hydrocarbon fractions in the soils mixed with different Fe^{2+}-containing materials at various H_2O_2 doses

Treatment	Fe^{2+} source	H_2O_2 dose	C16-C21	C21-C35	C35-C40
CFS	$FeSO_4{\cdot}7H_2O$	0% H_2O_2	5200±0a	18000±0b	2800±0a
T1FS	$FeSO_4{\cdot}7H_2O$	0.5% H_2O_2	3733±88c	14667±667cd	1967±67c
T2FS	$FeSO_4{\cdot}7H_2O$	1.0% H_2O_2	2433±133d	12667±882e	1733±33d
T3FS	$FeSO_4{\cdot}7H_2O$	1.5% H_2O_2	950±27g	8533±669fg	1533±120d
CM	Fe_3O_4	0% H_2O_2	5200±0a	21000±0a	2700±0a
T1M	Fe_3O_4	0.5% H_2O_2	4233±88b	15000±1528c	1733±88d
T2M	Fe_3O_4	1.0% H_2O_2	2600±173d	12967±33de	1600±100d
T3M	Fe_3O_4	1.5% H_2O_2	1400±200f	8400±200g	1700±58d
CP	FeS_2	0% H_2O_2	5300±0a	18000±0b	2700±0a
T1P	FeS_2	0.5% H_2O_2	4893±321a	15000±577c	2380±92b
T2P	FeS_2	1.0% H_2O_2	1933±33e	13400±265cde	2100±58c
T3P	FeS_2	1.5% H_2O_2	1300±153fg	10300±351f	2000±58c

All values are presented as mean ± standard error (n=3) and different letters in the same column indicate significantly different (p< 0.05).

For the C21-C35 fraction, the value in the control was significantly higher in the magnetite-treated soil than in the ferrous iron-treated and pyrite-treated soils. However, at 0.5% and 1% H_2O_2 doses, there was no significant difference among the three Fe^{2+} sources. At the highest H_2O_2 dose (1.5%), the residual hydrocarbon was higher in pyrite treatment than in the magnetite treatment.

Overall, there was a clear trend showing that the residual hydrocarbon decreased significantly with increasing H_2O_2 dose for all the three ferrous iron sources (Table 3).

Like the C16-C21 fraction, there was no significant difference among the three controls (CFS, CP and CM) for the C35-C40 fraction. However, for the 0.5% H_2O_2 dose, the residual hydrocarbon showed the following decreasing order: T1P > T1FS > T1M. There was no significant difference in residual hydrocarbon between the two higher H_2O_2 doses (1.0% and 1.5%) for all the three ferrous iron sources. By comparison, the concentration of residual hydrocarbon tended to be higher in pyrite treatment than in the other two ferrous iron sources (significant at $p<0.05$) (Table 3).

3.2 Various Residual Aromatic Hydrocarbons Using Different Fe^{2+} source

The concentration of the C10-C12 fraction tended to be higher in the pyrite treatment system than in the other two systems for any of the three levels of H_2O_2 doses with statistically significant difference being observed for most of the situations (Table 4).

Table 4 Concentration of various residual aromatic hydrocarbon fractions in the soils mixed with different Fe^{2+}-containing materials at various H_2O_2 doses

Treatment	Fe^{2+} source	H_2O_2 dose	C10-C12	C12-C16	C16-C21
CFS	$FeSO_4{\cdot}7H_2O$	0% H_2O_2	9000±0b	9700±0a	5700±0a
T1FS	$FeSO_4{\cdot}7H_2O$	0.5% H_2O_2	4167±88cd	4367±67d	4367±240c
T2FS	$FeSO_4{\cdot}7H_2O$	1.0% H_2O_2	1467±33h	3700±58de	3133±67e
T3FS	$FeSO_4{\cdot}7H_2O$	1.5% H_2O_2	1233±33h	3033±145e	2000±116f
CM	Fe_3O_4	0% H_2O_2	8600±0b	9400±0a	5700±0a
T1M	Fe_3O_4	0.5% H_2O_2	3900±58de	6333±674c	5467±67a
T2M	Fe_3O_4	1.0% H_2O_2	3393±299f	5500±231c	4633±88c
T3M	Fe_3O_4	1.5% H_2O_2	1500±361h	3033±88e	2267±120f
CP	FeS_2	0% H_2O_2	9600±0a	9700±0a	5100±0b
T1P	FeS_2	0.5% H_2O_2	4383±93c	7433±561b	4033±203d
T2P	FeS_2	1.0% H_2O_2	3600±58ef	6233±88c	817±55g
T3P	FeS_2	1.5% H_2O_2	2200±153g	1643±202f	383±92h

All values are presented as mean ± standard error (n=3) and different letters in the same column indicate significantly different ($p< 0.05$).

For the C12-C16 fraction, there was no significant difference among the three controls. While the concentration of residual hydrocarbon tended to be higher in the pyrite system than in the two

other systems at the H_2O_2 dose of 0.5% and 1.0%, the opposite was observed at the H_2O_2 dose of 1.5%, showing that the concentration of residual hydrocarbon was significantly lower in the pyrite system than in the other two systems (Table 4).

In contrast with C10-C12 fraction, the concentration of C16-C21 fraction tended to be significantly lower in the pyrite system than in the other two systems at any of the H_2O_2 dosage levels (Table 4).

3.3 Various Residual Aliphatic Hydrocarbons under Different Temperature and Salinity Conditions

In general, the concentration of aliphatic hydrocarbon was significantly lower in the treatment than in its respective control for all the three fractions (C16-C21, C21-C35 and C35-C40). However, different distribution patterns were observed for each individual fraction. For the C16-C21 fraction, there was no significant difference among the four controls. At the same temperature condition, the concentration of residual hydrocarbon was lower at the lower salinity level than at the higher salinity level. At the same salinity level, the concentration of residual hydrocarbon was lower at a lower temperature than at a higher temperature (Fig. 1a).

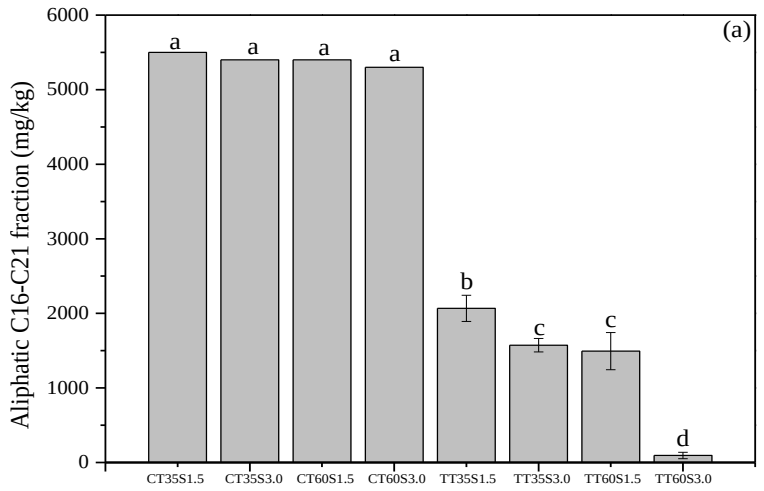

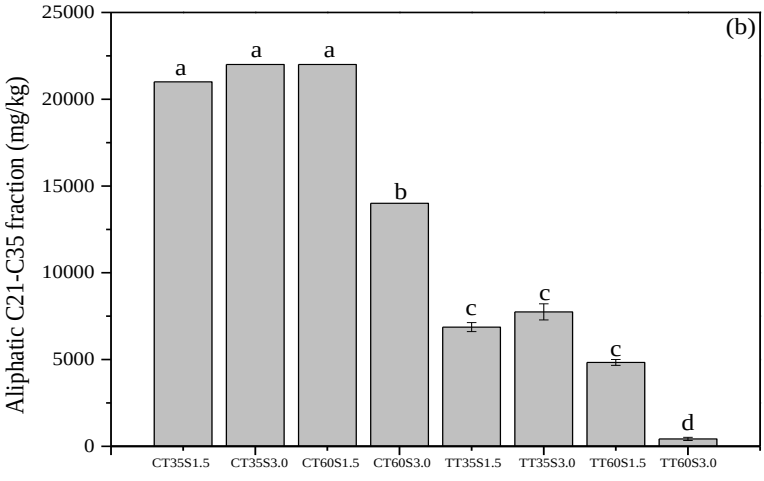

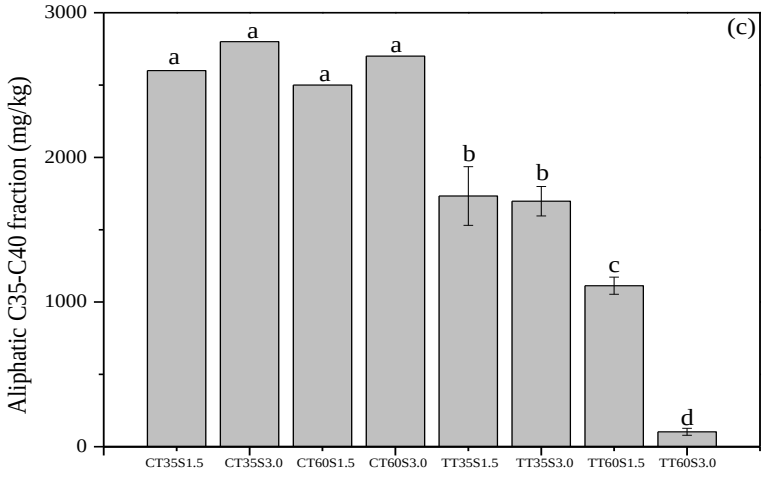

Figure 1 Various soil-borne aliphatic petroleum hydrocarbon fractions in the controls and different combined temperature-salinity treatments. (a) C16-C21 fraction, (b) C21-C35 fraction, (c) C35-C40 fraction. All values are presented as mean ± standard error (n=3) and bars with different letters indicate significantly different ($p < 0.05$).

For the C21-C35 fraction, the concentration of hydrocarbon was significantly lower in CT60S3.0 than in other controls. There was no significant difference in residual hydrocarbon among TT35S1.5, TT35S3.0 and TT60S1.5. However, TT60S3.0 was significantly lower than any other treatments (Fig. 1b).

For the C35-C40 fraction, there was no significant difference among the four controls. At the same salinity level, the concentration of residual hydrocarbon was lower at 60^{o}C than at 35^{o}C. There was no significant difference in the residual hydrocarbon between the two 35^{o}C treatments with different salinity. However, for the two 60^{o}C treatments, the residual hydrocarbon concentration was lower at the higher salinity than at the lower salinity (Fig. 1c).

3.4 Various Residual Aromatic Hydrocarbons under Different Temperature and Salinity Conditions

There was no significant difference among the four controls for any of the aromatic hydrocarbon fractions. For C10-C12 fraction, no residual hydrocarbon was detected for all the treatments (Fig. 2a).

For the C12-C16 fraction, there was no significant difference in residual hydrocarbon between the two 35^{o}C treatments with different level of salinity. The concentration of residual hydrocarbon was lower in the 60^{o}C treatments than in the 35^{o}C treatments. For the 60^{o}C treatments, the concentration of residual hydrocarbon was much lower at higher salinity than at the lower salinity (significant at $p<0.05$) (Fig. 2b).

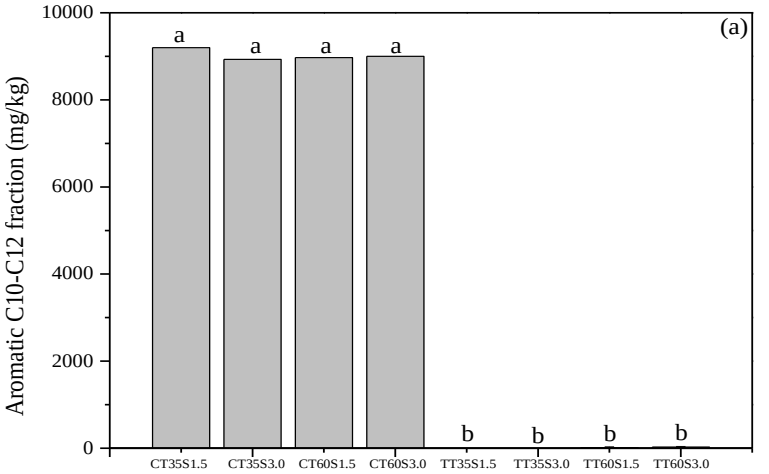

199

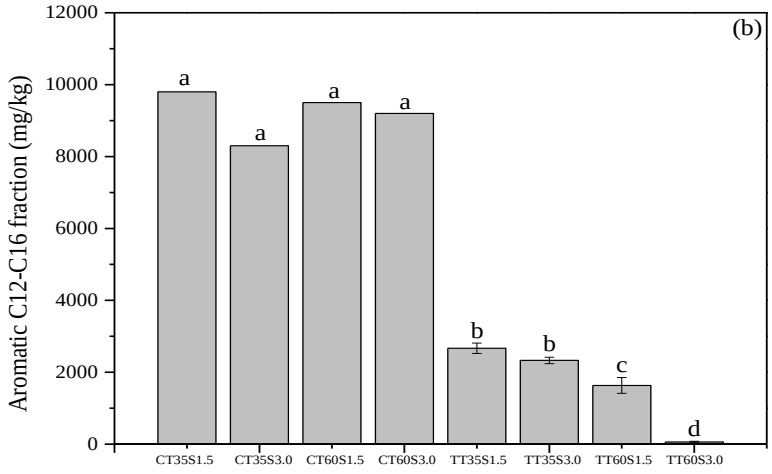

200

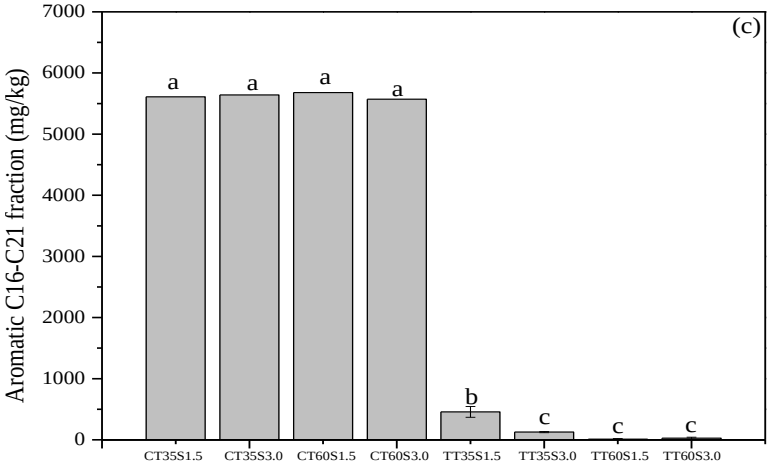

201

202 **Figure 2 Various soil-borne aromatic petroleum hydrocarbon fractions in the controls and**
203 **different combined temperature-salinity treatments. (a) C10-C12 fraction, (b) C12-C16**
204 **fraction, (c) C16-C21 fraction. All values are presented as mean ± standard error (n=3) and**
205 **bars with different letters indicate significantly different ($p < 0.05$).**

For the C16-C21 fraction, residual hydrocarbon under 60^{o}C treatments was not detected. For the 35^{o}C treatments, the concentration of residual hydrocarbon was lower at the higher salinity level than at the lower salinity level (Fig. 2c).

4 Discussion

Under the set experimental conditions, the maximum decomposition rate of petroleum hydrocarbons was achieved at the highest dose of H_2O_2 (1.5%). At this dosage level, over 70%, 50% and 25% of aliphatic C16-C21, C21-C35 and C35-C40, respectively, was eliminated, depending on the type of ferrous iron-containing materials being used to trigger the Fenton reaction (Table 3). The decreasing removal rate with increasing length of carbon chain is expected since larger petroleum hydrocarbon molecules tend to be more resistant to chemical attack (Waples, 1985; Rothermich et al., 2002; Khan et al., 2004). Despite that ferrous sulfate is a water-soluble chemical and, in theory, its rapid release of dissolved Fe^{2+} could be favourable for hydroxyl radical generation through Fenton reaction, it did not exhibit a significantly stronger capacity to decompose the petroleum hydrocarbons, as compared to magnetite. Possibly, oxidation of ferrous iron prior to Fenton-like reaction resulted in a reduction of Fe^{2+} availability (Minegishi et al., 1983). The oxidation of Fe^{2+} can be accelerated under alkaline conditions (Hove et al., 2007; Daenzer et al., 2015) such as those encountered in desert soils and this could further weaken its availability. Therefore, the use of magnetite that is usually much cheaper than ferrous sulfate has the advantage over the use of ferrous sulfate as a source of Fe^{2+} for triggering Fenton-like reaction. The relatively lower removal rate of aliphatic hydrocarbons in the pyrite system was likely due to the competition of reduced sulfur species contained in pyrite with the ferrous iron for the available H_2O_2 and possibly hydroxyl radical as well (Ma et al., 2013). This could reduce the amount of hydroxyl radical available for decomposing the hydrocarbons.

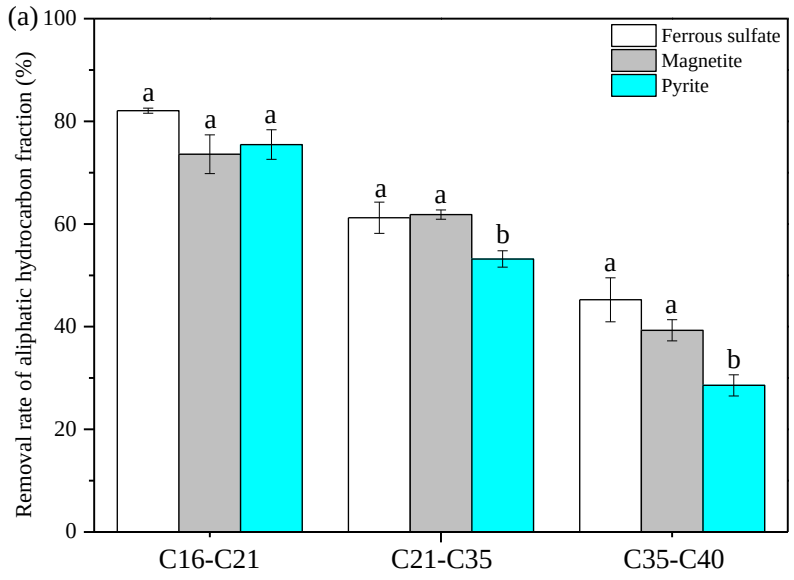

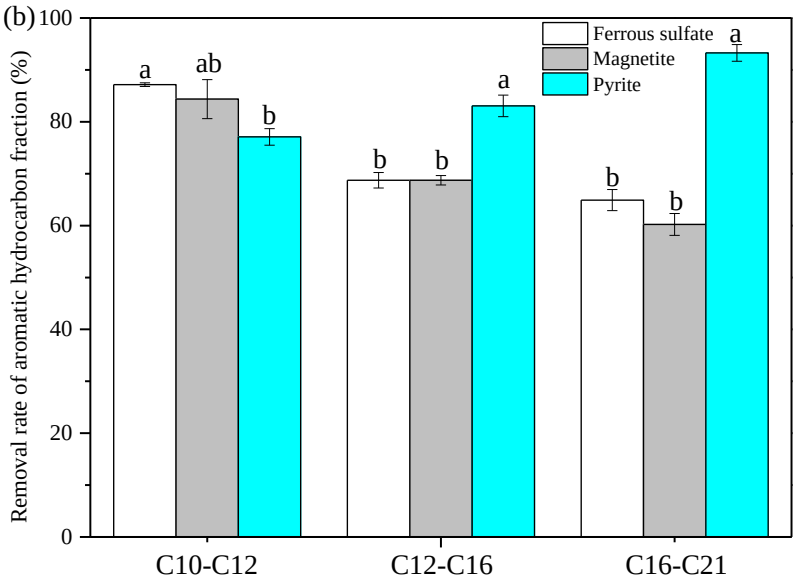

Figure 3 Comparison of removal rate for (a) aliphatic hydrocarbons and (b) aromatic hydrocarbons among the treatments with the three different ferrous iron-containing materials

It is interesting to note that while there was a trend showing the decomposition rate of aromatic hydrocarbons decreased with increasing length of carbon chain in the ferrous sulfate and magnetite systems, the opposite was observed in the pyrite system where the decomposition rate of aromatic hydrocarbons increased with increasing length of carbon chain (Table 3). This may be attributed to the strong capacity of pyrite-induced Fenton process to destroy aromatic ring (Zhang et al., 2014).

With the same carbon range (i.e. C16-C21), the removal rate tended to be higher for aliphatic hydrocarbons than for aromatic hydrocarbons in the ferrous sulfate and magnetite systems.

Apart from the generally poorer performance of ferrous sulfate and pyrite relative to magnetite in terms of decomposing the long-chain petroleum hydrocarbons, the formers are hazardous materials that require careful handling while the latter is generally viewed as harmless or less harmful material. It is therefore reasonable to select magnetite as a source of ferrous iron for advanced oxidation of long-chain petroleum hydrocarbons.

While it is generally believed that Fenton reaction is accelerated by increase in temperature (Neyens et al., 2003; Zapata et al., 2010; Díaz de Tuesta et al., 2015), the effectiveness of Fenton-driven degradation of organic molecules may be affected due to enhanced decomposition of H_2O_2 under high temperature conditions (Lee et al., 2003; Malik et al., 2003; Rodriguez et al., 2003; Lopez et al., 2005; Gulkaya et al., 2006; Alaton et al., 2007). Aygun et al. (2012) found that the landfill leachate can be most effectively removed by Fenton reaction at around 35^{o}C. However, the work by Khamaruddin et al. (2011) showed that degradation rate of diisopropanolamine by Fenton process increased with increasing temperature up to 60^{o}C. The enhanced effects of Fenton process on degradation of long-chain petroleum hydrocarbons by increased temperature observed in this study suggests that at a temperature of 60^{o}C, the enhancement of Fenton process outweighed the adverse effects from potential loss of H_2O_2 due to elevated temperature when the Fenton process is applied to treatment of long-chain petroleum hydrocarbons.

Bacardit et al. (2007) showed that the overall TOC removal by photo-Fenton process was not influenced by the presence of chloride, but the process becomes much slower. This was in contrast with our results showing that the decomposition of soil-borne petroleum hydrocarbons was not impeded in the presence of sodium chloride. Lu et al. (2005) suggested that the inhibition of aniline oxidation by Fenton's reagent was due to complexation of chloride ion with water-borne Fe^{2+},

reducing the availability of Fe^{2+} for Fenton reaction. In our experiment, solid-borne Fe^{2+} (magnetite) was used, which could prevent consumption of Fe^{2+} by complexation with chloride ion from occurring. This could effectively eliminate the inhibitory effect of chloride on Fenton reaction. In fact, the removal rate of aliphatic hydrocarbons in our experiment even tended to be higher at a higher salinity when the temperature was 60^{o}C and the removal rate of aromatic hydrocarbons tended to be higher at a higher salinity when the temperature was 35^{o}C. The reason for this is unclear and further investigation is required to gain insights into the mechanism behind the observed phenomenon.

While it is expected that a higher dosage level of H_2O_2 could result in higher decomposition rate of the petroleum hydrocarbons, the use of H_2O_2 at a concentration of 1.5% is deemed to be more appropriate for safe on-ground soil treatment operation purposes (Kalloo et al., 1997; Young et al., 2003). This also considers the special climatic conditions in desert areas where the soil moisture content tends to be very low and therefore requires a larger volume of liquid to be added into the contaminated soils to ensure sufficient contact between the hydroxyl radical and the petroleum hydrocarbons. An increase in concentration of H_2O_2 will markedly increase the treatment costs, which could outweigh the potential benefit from the enhanced removal rate of soil-borne petroleum hydrocarbons. The use of a low dose of H_2O_2 can be further justified by the fact that desert soils frequently contain only a limited amount of organic matter. The presence of soil organic matter could strongly compete with the petroleum hydrocarbons for the available hydroxyl radical generated from Fenton-like reaction (Wang et al., 2015). The organic matter-deficient nature of desert soils means that competitive consumption of hydroxyl radical by this consumer is limited.

The findings obtained from this study have implications for developing cost-effective strategies to remediate aged crude oil-contaminated soils in desert areas such as the widespread oil-contaminated soils in Kuwait that were resulted from the first Gulf War. Following the weathering

for over two decades, the volatile component of the crude oil has been translocated into atmosphere, resulting in that the long-chain species dominated in the soil-borne petroleum hydrocarbons. This area has an average annual rainfall of less than 150 mm and an average maximum temperature range of 40-46^{o}C during the period from May to September. Saline soils are common in this area with some of the soils having an electrical conductivity greater than 10 dS/m (our unpublished data). The discovery that high soil temperature and salinity did not adversely affect the chemical oxidation of the long-chain petroleum hydrocarbons suggests that proposed advanced oxidation method is suitable for being used in the Kuwaiti oil lake areas. Based on current market price, the costs for the materials needed to treat aged crude oil-contaminated soils with a total petroleum hydrocarbon about 5% in the desert areas are less than US$45 per ton. This chemical treatment results in no generation of known toxic substances that could adversely affect the growth of petroleum hydrocarbon-degrading microbes. Therefore, the advanced oxidation method developed in this work can serve as the pre-treatment step for the follow-up bioremediation as long as favourable environmental conditions are created to meet the growth requirements for hydrocarbon-degraders (Xu et al., 2011).

5 Conclusion

The decomposition rate of petroleum hydrocarbons was similar to each other for ferrous sulfate and magnetite reaction systems. But the capacity of pyrite to trigger Fenton-driven decomposition of long-chain aliphatic petroleum hydrocarbons was weaker, as compared to ferrous sulfate and magnetite. The degradation rate of aromatic hydrocarbons decreased with increasing length of carbon chain in the ferrous sulfate and magnetite systems. However, the opposite was observed in the pyrite system. The effect of Fenton process on degradation of long-chain petroleum hydrocarbons was enhanced by increased temperature. At a temperature of 60^{o}C, the enhancement of Fenton process outweighed the adverse effects from potential loss of H_2O_2 due to elevated temperature. The use of magnetite as a source of ferrous iron was likely to prevent consumption of Fe^{2+} by

complexation with chloride ion from occurring and consequently effectively eliminated the inhibitory effect of salinity on Fenton reaction.

Acknowledgements

The petroleum hydrocarbon analysis was performed in the accredited commercial analytical laboratory operated by the Concept Life Sciences Analytical & Development Services Limited, Manchester, England.

References

Alaton, I.A., Teksoy, S., 2007. Acid dyebath effluent pretreatment using Fenton's reagent: Process optimization, reaction kinetics and effects on acute toxicity. Dyes. Pigments. 73, 31-39.

Aygun, A., Yilmaz, T., Nas, B., Berktay, A., 2012. Effect of temperature on fenton oxidation of young landfill leachate: Kinetic assessment and sludge properties. Global. NEST. J. 14, 487-495.

Bissey, L.L., Smith, J.L., Watts, R.J., 2006. Soil organic matter–hydrogen peroxide dynamics in the treatment of contaminated soils and groundwater using catalyzed H_2O_2 propagations (Modified Fenton's Reagent). Water. Res. 40, 2477-2484.

Bacardit, J., Stötzner, J., Chamarro, E., Esplugas, S., 2007. Effect of salinity on the photo-Fenton process. Ind. Eng. Chem. Res. 46, 7615-7619.

Bach, A., Shemer, H., Semiat, R., 2010. Kinetics of phenol mineralization by Fenton-like oxidation. Desalination 264, 188-192.

Daenzer, R., Feldmann, T., Demopoulos, G.P., 2015. Oxidation of ferrous sulfate hydrolyzed slurry kinetic aspects and impact on As (V) removal. Ind. Eng. Chem. Res. 54, 1738-1747.

Díaz de Tuesta, J.L., García- Figueruelo, C., Quintanilla, A., Casas, J.A., Rodriguez, J.J., 2015. Application of high- temperature Fenton oxidation for the treatment of sulfonation plant wastewater. J. Chem. Technol. Biotechnol. 90, 1839-1846.

Gulkaya, I., Surucu, G.A., Dilek, F.B., 2006. Importance of H_2O_2/Fe^{2+} ratio in Fenton's treatment of a carpet dyeing wastewater. J. Hazard. Mater. 136, 763-769.

Hall, C., Tharakan, P., Hallock, J., Cleveland, C., Jefferson, M., 2003. Hydrocarbons and the evolution of human culture. Nature 426, 318-322.

Hove, M., van Hille, R.P., Lewis, A.E., 2007. Iron solids formed from oxidation precipitation of ferrous sulfate solutions. AIChE J. 53, 2569-2577.

Kalloo, A.N., Canto, M., Smith, C., Wadwa, K.S., Pasricha, P.J., 1997. Hydrogen peroxide (3%) is safe and effective in the endoscopic visualization of bleeding lesions in patients with acute upper gastrointestinal bleeding (UGIB). Gastrointest. Endo. 45, AB93.

Khan, F.I., Husain, T., Hejazi, R., 2004. An overview and analysis of site remediation technologies. J. Environ. Manage. 71, 95-122.

Khamaruddin, P.F., Bustam, M.A., Omar, A. A., 2011.Using Fenton's reagents for the degradation of diisopropanolamine: effect of temperature and pH. International Conference on Environment and Industrial Innovation IPCBEE 12, IACSIT Press, Singapore.

Lee, Y., Lee, C., Yoon, J., 2003. High temperature dependence of 2, 4-dichlorophenoxyacetic acid degradation by Fe^{3+}/H_2O_2 system. Chemosphere 51, 963-971.

Lopez, A., Mascolo, G., Detomaso, A., Lovecchio, G., Villani, G., 2005. Temperature activated degradation (mineralization) of 4-chloro-3-methyl phenol by Fenton's reagent. Chemosphere 59, 397-403.

354 Lu, M.C., Chang, Y.F., Chen, I.M., Huang, Y.Y., 2005. Effect of chloride ions on the oxidation of
355 aniline by Fenton's reagent. J. Environ. Manage. 75, 177-182.

356 Li, X.J., Zhao, Q., Wang, X., Li, Y.T., Zhou, Q.X., 2018. Surfactants selectively reallocated the
357 bacterial distribution in soil bioelectrochemical remediation of petroleum hydrocarbons. J.
358 Hazard. Mater. 344, 23-32.

359 Ma, Y.Q., Lin, C.X., 2013. Microbial oxidation of Fe^{2+} and pyrite exposed to flux of micromolar
360 H_2O_2 in acidic media. Sci. Rep. 3, 1979.

361 Margesin, R., Schinner, F., 2001. Biodegradation and bioremediation of hydrocarbons in extreme
362 environments. Appl. Microbiol. Biot. 56, 650-660.

363 Malik, P., Saha, S., 2003. Oxidation of direct dyes with hydrogen peroxide using ferrous Ion as
364 catalyst. Sep. Purif. Technol. 31, 241-250.

365 Maizel, A.C., Remucal, C.K., 2017. The effect of advanced secondary municipal wastewater
366 treatment on the molecular composition of dissolved organic matter. Water. Res. 122, 42-52.

367 Minegishi, T. Asaki, Z., Higuchi, B., Kondo, Y., 1983. Oxidation of ferrous sulfate in weakly acidic
368 solution by gas bubbling. Metallurgical Transactions B. 14, 17-24.

369 Neyens, E., Baeyens, J., 2003. A review of classic Fenton's peroxidation as an advanced oxidation
370 technique. J. Hazard. Mater. B98, 33-50.

371 Rhykerd, R.L., Weaver, R.W., McInnes, K.J., 1995. Influence of salinity on bioremediation of oil in
372 soil. Environ. Pollut. 90, 127-130.

373 Rothermich, M.M., Hayes, L.A., Lovley, D.R., 2002. Anaerobic, sulfate-dependent degradation of
374 polycyclic aromatic hydrocarbons in petroleum-contaminated harbor sediment. Environ. Sci.
375 Technol. 36, 4811-4817.

376 Rodriguez, M.L., Timokhin, V.I., Contreras, S., Chamarro, E., Esplugas, S., 2003. Rate equation for
377 the degradation of nitrobenzene by 'Fenton-like'reagent. Adv. Environ. Res. 7, 583-595.

378 Safdari, M.S., Kariminia, H.R., Rahmati, M., Fazlollahi, F., Polasko, A., Mahendra, S., Wilding,
379 W.V., Fletcher, T.H., 2018. Development of bioreactors for comparative study of natural
380 attenuation, biostimulation, and bioaugmentation of petroleum-hydrocarbon contaminated soil.
381 J. Hazard. Mater. 342, 270-278.

382 Vieira, P.A., Vieira, R.B., de Franca, F.P., Cardoso, V.L., 2007. Biodegradation of effluent
383 contaminated with diesel fuel and gasoline. J. Hazard. Mater. 140, 52-59.

384 Varjani, S.J., 2017. Microbial degradation of petroleum hydrocarbons. Bioresource. Technol. 233,
385 277-286.

386 Waples, D.W., 1985. Geochemistry in petroleum exploration. International Human Resources
387 Development Corporation. Boston, pp232.

388 Wang, W., Xu, J.L., Huang, F.D, Cui, Y.W., 2015. Hydrogen peroxide (H_2O_2) requirement for the
389 oxidation of crude oil in contaminated soils by a modified Fenton's reagent. Toxico. Enviro.
390 Chem. 97, 275-281.

391 Weisman, W., 1998. Analysis of petroleum hydrocarbons in environmental media. Amherst
392 Scientific Publishers. MA, pp98.

393 Xu, J., Xin, L., Huang, T., Chang, K., 2011. Enhanced bioremediation of oil contaminated soil by
394 graded modified Fenton oxidation. J. Environ. Sci. 23, 1873-1879.

395 Young, J.A., 2003. Hydrogen peroxide, 3%. J. Chem. Educ. 80, 1132.

396 Zapata, A., Oller, I., Rizzo, L., Hilgert, S., Maldonado, M.I., Sánchez-Pérez, J.A., Malato, S., 2010.
397 Evaluation of operating parameters involved in solar photo-Fenton treatment of wastewater:

Interdependence of initial pollutant concentration, temperature and iron concentration. Appl. Catalysis B: Environ. 97, 292-298.

Zhang, Y.L., Zhang, K., Dai, C.M., Zhou, X.F., Si, H.P., 2014. An enhanced Fenton reaction catalyzed by natural heterogeneous pyrite for nitrobenzene degradation in an aqueous solution. Chem. Eng. J. 244, 438-445.

Zhu, H., Taylor, A.A., Astor, S.R., Terry, N., 2017. Enhancing saltgrass germination and growth in a saline soil contaminated with petroleum hydrocarbons. Plant. Soil. 412, 189-199.

Figure Captions

Figure 1 Various soil-borne aliphatic petroleum hydrocarbon fractions in the controls and different combined temperature-salinity treatments. (a) C16-C21 fraction, (b) C21-C35 fraction, (c) C35-C40 fraction. All values are presented as mean ± standard error (n=3) and bars with different letters indicate significantly different ($p< 0.05$).

Figure 2 Various soil-borne aromatic petroleum hydrocarbon fractions in the controls and different combined temperature-salinity treatments. (a) C10-C12 fraction, (b) C12-C16 fraction, (c) C16-C21 fraction. All values are presented as mean ± standard error (n=3) and bars with different letters indicate significantly different ($p< 0.05$).

Figure 3 Comparison of removal rate for (a) aliphatic hydrocarbons and (b) aromatic hydrocarbons among the treatments with the three different ferrous iron-containing materials